Volume 18, Number 5, 2025. pp. 695-703

Jordan Journal of Physics

ARTICLE

Soil Radioactivity Levels, Spatial Distribution and Radiation Hazard Assessment in Anambra and Imo States, Southeastern Nigeria

O. I. Agbelusi[a], P. S. Ayanlola[b], M. K. Lawal[c], S. O. Awokoya[b], O. O. Oloyede[b], A. Olatunji[d] and G. A. Isola[b]

[a] *Department of Physical Sciences, Chrisland University, Abeokuta, Nigeria.*

[b] *Department of Pure and Applied Physics, Ladoke Akintola University of Technology, Ogbomoso, Nigeria.*

[c] *Department of Science Laboratory Technology, Ladoke Akintola University of Technology, Ogbomoso, Nigeria..*

[d] *Department of Physics, Ajayi Crowther University, Oyo, Nigeria.*

Doi: **https://doi.org/10.47011/18.5.10**

Received on: 27/01/2025; *Accepted on: 07/04/2025*

Abstract: This study assessed the radioactivity levels in soil samples from Anambra and Imo States, two regions affected by the Nigerian Civil War. Using a thallium-activated sodium iodide detector, a total of 80 stratified, randomly collected soil samples were analyzed. The detected radionuclides included non-serial ^{40}K and decay series of ^{238}U and ^{232}Th, as well as trace levels of the anthropogenic ^{137}Cs. Their spatial variability and associated health implications were also evaluated. The average activity concentrations in Anambra State were 835.91 ± 7.40 Bq kg^{-1} for ^{40}K, 21.05 ± 3.65 Bq kg^{-1} for ^{238}U, 12.99 ± 0.85 Bq kg^{-1} for ^{232}Th, and 3.88 ± 0.10 Bq kg^{-1} for ^{137}Cs. In Imo State, the respective values were 761.29 ± 6.63, 19.19 ± 2.97, 9.29 ± 1.52, and 5.39 ± 0.25 Bq kg^{-1}. The estimated mean absorbed dose rates were 52.65 nGyh^{-1} for Anambra and 46.38 nGyh^{-1} for Imo, corresponding to annual effective dose equivalents of 0.06 mSvy^{-1} for both states, a value well below the global safety thresholds. Spatial analysis revealed that ^{40}K levels were influenced by potassium-rich soils and intensive agricultural practices, while geological formations governed the distribution of ^{238}U and ^{232}Th. This study confirms that current soil usage poses no immediate radiological risks. However, proactive monitoring is recommended to mitigate potential long-term radiological impacts.

Keywords: Soil radioactivity, Spatial distribution, Radiation hazard, Gamma spectrometry, Nigeria.

1. Introduction

Human exposure to naturally occurring radioactive materials (NORM) is an inevitable aspect of everyday life. Primordial radionuclides such as ^{238}U, ^{232}Th, along with radon isotopes (^{222}Rn) from the decay of these elements and the non-serial decay ^{40}K, are the primary sources of natural radiation. While the radiation from these sources is universal, the risks associated with ionizing radiation vary depending on the region's geological setting, human activities, and historical factors [1-4]. Therefore, global background radiation levels differ significantly. Thus, the understanding of these concentrations is essential in quantifying the absorbed dose and potential radiological hazards, which can have significant public health implications [5-9].

Several studies from various parts of the world have been carried out to assess the radionuclide levels of different environmental matrices, most especially soil. In the study conducted by Leal *et al.* [8], it was reported that the median values of the activity concentrations

Corresponding Author: P. S. Ayanlola **Email**: psayanlola28@lautech.edu.ng

of ^{226}Ra, ^{228}Ra, and ^{40}K in the soils of Pernambuco, Brazil, were consistent with values reported worldwide. In reporting their findings on the natural radioactivity in soil dust samples from Ketu, Ghana, Addo *et al.* [10] found that the soils in the studied area had normal levels of radiation and were therefore radiologically safe. In another study conducted by Nagathil *et al.* [11] to investigate the spatial analysis of radionuclide concentration in the high background radiation regions of Kerala, India, it was reported that the results obtained exceed the safe limits recommended by the [1]. Abu-Kharma *et al.* [12] reported that, with the exception of ^{40}K and ^{232}Th, the radioactivity levels obtained for ^{238}U in soils from Al-Lajjun, Jordan, were significantly higher than world average values.

In Southern Nigeria, Anambra and Imo states were among the regions severely affected by the Nigerian Civil War waged half a century ago (1967 - 1970). As radiation exposure is influenced by both natural and anthropogenic factors, the movement of contaminated soil and debris in the zones can contribute to elevated radiation levels. While examining the radioactivity levels and related radiological dangers of surface soils in Ore metropolis, Ondo state, Nigeria, a town located along the civil war track, Akinloye *et al.* [13] reported the presence of primordial radionuclides and detected ^{137}Cs at three places. Furthermore, after evaluating the radioactive contents in soil and food samples in Enugu state, southeastern Nigeria, Agbelusi *et al.* [14] found that the radioactivity levels and calculated radiological indices were above the prescribed limits. The results also revealed that ^{137}Cs were present in a small number of communities at low concentrations, which was linked to wartime activity.

Hence, the redistribution of artificial radionuclides during this period, in conjunction with natural radiation sources, has raised concerns about long-term exposure risks in other regions (specifically Anambra and Imo states) affected by the war. Soils, frequently used for construction and agricultural purposes, are a significant source of both external gamma radiation and internal radon exposure. The accumulation of the penetrative radiations in poorly ventilated buildings may further elevate internal radiation exposure, making this a public health concern. Epidemiological studies have linked prolonged exposure to natural radionuclides to severe health issues [15, 16]. The health risks associated with ionizing radiation include genetic damage and other conditions such as tumors, cataracts, and leukemia.

This study, therefore, focuses on evaluating the levels of radionuclides in Anambra and Imo states, offering a comprehensive assessment of the associated health impacts, as well as identifying and mapping radiation hotspots. Particular attention is given to areas where elevated radiation levels are influenced by both natural sources and the historical redistribution of radioactive materials. The study aims to contribute to public health initiatives by providing baseline data for radiation monitoring in the states, with emphasis on the spatial distribution of radionuclides. The findings are expected to support the development of radiation protection programs, inform policymakers about radiation-related risks, and aid efforts to mitigate exposure in both urban and rural areas. In addition, this research provides a foundation for future studies on radiation hazards in Anambra and Imo States. Overall, the study aligns with the United Nations Sustainable Development Goals by contributing to the promotion of healthy lives and well-being for all at all ages (SDG 3) and to the development of inclusive, safe, resilient, and sustainable cities and human settlements (SDG 11) [17].

2. Materials and Methods

2.1 Study Area

Anambra and Imo states, located in southeastern Nigeria (Fig. 1), are known for their rich cultural heritage and diverse socio-economic landscapes. Anambra State, nicknamed the Light of the Nation and one of the urbanized states in Nigeria, lies between latitudes 5°50'N and 7°10'N and longitudes 6°40'E and 7°25'E, with a land area of approximately 4,844 km². It is the eighth most populous state in the country and the second most densely populated after Lagos State, with a population exceeding 7.2 million. Anambra experiences a tropical wet-and-dry (savanna) climate, with an average annual temperature of about 28.99 °C, which is slightly lower than the national average. The state receives approximately 212.36 mm (8.36 inches) of rainfall annually and experiences rainfall on

about 243 days per year, corresponding to roughly 66.7% of the year.

Imo state, positioned between latitudes 4°45'N and 7°15'N and longitudes 6°50'E and 7°25'E, covers a total area of 5530 km^2. Although it is the third smallest state in Nigeria by area, Imo State is the fourteenth most populous, with an estimated population exceeding 6 million as of 2022 [18, 19]. Both states are adjacent to each other and have predominantly agrarian economies, with farming and trading as common occupations.

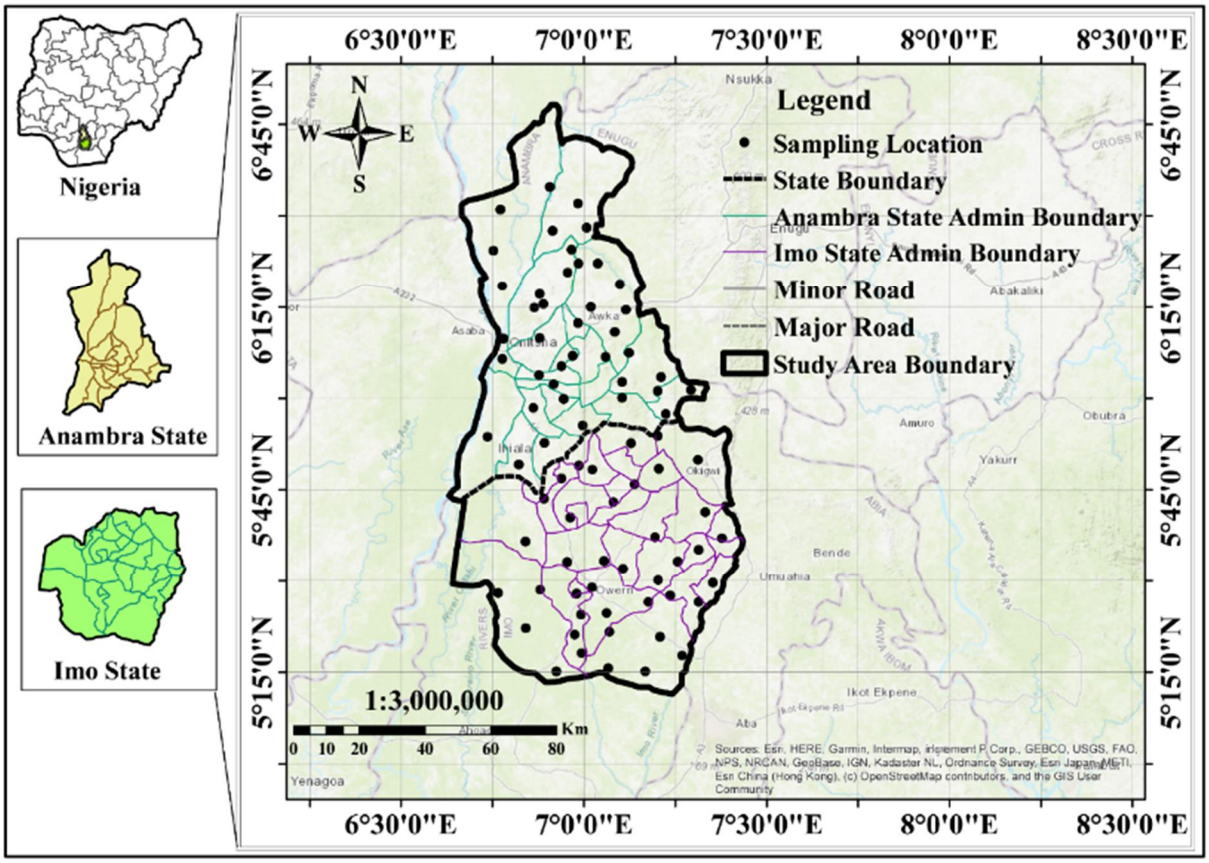

FIG. 1. Map of study area.

2.2 Sample Collection

An initial survey was conducted to identify representative sampling points across the study area. Subsequently, the study area was divided into four regions covering the northern and southern parts of each state, with random sampling points selected within each region to ensure spatial variability and adequate coverage of the entire area. Soil samples were collected using a hand auger to a depth of 10 cm. A total of 80 soil samples were collected from Anambra and Imo states and packaged in a black polypropylene bag pending laboratory preparation and spectrometry analysis.

2.3 Sample Preparation

The soil samples were air-dried at room temperature to a constant weight, ground up, and sieved through a 2 mm mesh. A 200 g portion of each sample was placed into a cylindrical polypropylene container that matched the detector's geometry and was tightly sealed to prevent ^{222}Rn from escaping. To ensure radioactive secular equilibrium between ^{238}U and its decay products, as well as between ^{232}Th and its progeny, all samples were stored for 28 days before being measured [2, 3].

2.4 Sample Measurement

The samples underwent gamma spectrometry analysis using a gamma spectrometry system that featured a 3" x 3" sodium iodide detector activated with thallium [NaI(Tl)], which was linked to a multichannel analyzer (MCA), specifically the GS-2000 Pro model. Acquisition and analysis of the gamma-ray spectra were carried out using Theremino software. The calibration of the system was accomplished using standard sources that contained known radionuclides, with an acquisition duration of 36000 s. Before measuring the samples, an

empty container identical in geometry to the detector was counted for 36000 s to determine the background gamma-ray distribution. After reaching secular equilibrium, the sealed samples were counted for the same period. The concentrations of radionuclides were estimated by analyzing the gamma energies of ^{214}Pb at 352.0 keV, ^{214}Bi at 609.3 keV for ^{238}U, ^{208}Tl at 583.2 keV, and ^{228}Ac at 911.1 keV for ^{232}Th, as well as ^{40}K at 1460.8 keV and ^{137}Cs at 661.6 keV [2, 3, 20]. The activity concentrations A (Bq kg^{-1}) of the samples were calculated using Eq. (1):

$$A\ (Bq\ kg^{-1}) = \frac{C_{net}}{\mathrm{P\gamma \times \varepsilon \times m \times t}} \quad (1)$$

where ε is the detector's full energy peak efficiency, t is the counting time, m is the sample mass, C_{net} is the net peak area, and P_γ is the absolute gamma-ray emission probability [2 - 4, 14, 20].

The minimum detectable activity (MDA) for each radionuclide was determined using Eq. (2):

$$MDA = \frac{2.71+4.66\ (\sigma)}{\mathrm{P\gamma \times \varepsilon \times m \times t}} \quad (2)$$

where Pγ, ε, m, and t remain as earlier defined, and σ is the standard deviation of the background recorded at time t over the energy range of interest. For ^{40}K, ^{238}U, ^{232}Th, and ^{137}Cs, the corresponding minimum detectable limit (MDA) is 7.79 Bq kg^{-1}, 5.68 Bq kg^{-1}, 4.59 Bq kg^{-1}, and 2.98 Bq kg^{-1}, respectively.

2.4.1 Calculation of Absorbed Dose Rate

Equation (3) was used to assess the contribution of the radionuclides found in the samples to the absorbed dose rate as a result of external exposure [1-4, 14, 20].

$$D\ (nGyh^{-1}) = 0.462\ A_u + (0.621\ A_{Th}) + (0.0417\ A_k) \quad (3)$$

where A_U, A_{Th}, and A_k are the activity concentrations of ^{238}U, ^{232}Th, and ^{40}K, respectively.

2.4.2 Calculation of Annual Effective Dose Equivalent

Equation (4) was used to estimate the annual effective dose equivalent caused by the radionuclides found in the soil samples:

$$AEDE\ (mSvy^{-1}) = D\ (nGyh^{-1}) \times 24hr \times 365.25days \times 0.2 \times 0.7(SvGy^{-1}) \times 10^{-6} \quad (4)$$

where 0.7 SvGy^{-1} is the conversion coefficient which transforms the absorbed dose rate in the air to an effective dose, and 10^{-6} is the factor converting nanosievert into millisievert [1-4, 14, 20].

2.4.3 Spatial Distribution of Soil Radioactivity Concentration

Using the spatial analyst extension in the geographic information system (GIS) environment, the spatial distribution of the radionuclide concentrations was carried out in ArcMap 10.8.2. Using the Kriging interpolation technique described by [21], a map of the distribution of activity concentration of detected radionuclides was created, offering a comprehensive view of the radionuclide distribution. This provides crucial insights into how local geological formations, agricultural activities, and historical events impact radionuclide concentrations.

3. Results and Discussion

Tables 1 and 2 present the results of the gamma spectrometry analysis of soil collected from Anambra and Imo states. In Anambra state, the activity concentrations of ^{40}K ranged from 42.44±6.72 to 2275.54±15.67 Bq kg^{-1}, with a mean of 835.91±7.40 Bq kg^{-1}. The activity concentrations of ^{238}U ranged from 9.09±3.67 to 57.56±3.52 Bq kg^{-1}, with a mean of 21.05±3.65 Bq kg^{-1}. For ^{232}Th, concentrations ranged from 4.78 ± 0.73 to 38.69±0.66 Bq kg^{-1}, with a mean of 12.99±0.85 Bq kg^{-1}. Additionally, the ^{137}Cs concentrations ranged from 3.66±0.10 to 4.16±0.20 Bq kg^{-1}, with a mean of 3.88±0.10 Bq kg^{-1}. In Imo state, the activity concentrations of ^{40}K ranged from 106.01 ± 1.76 to 2135.74±18.37 Bq kg^{-1}, with a mean of 761.29±6.63 Bq kg^{-1}. The concentrations of ^{238}U ranged from 10.01±1.92 to 34.44±1.37 Bq kg^{-1}, with a mean of 19.19±2.97. The concentrations of ^{232}Th ranged from 4.96±0.42 to 15.43±4.03 Bq kg^{-1} with a mean of 9.29±1.52. Similarly, ^{137}Cs concentrations ranged from 3.76±0.11 to 4.78±0.23 Bq kg^{-1}, with a mean of 5.39±0.25 Bq kg^{-1}. These values are significantly lower than the global average of 400.00, 35.00, 30.00, and 10.00 Bq kg^{-1} for ^{40}K, ^{238}U, ^{232}Th, and ^{137}Cs, respectively [1]. However, Anambra state recorded higher radionuclide levels than Imo State. These elevated levels can be attributed to a combination of the region's geological composition and significant industrial activities. Geologically, Anambra is characterized by formations rich in NORMs, such as granitic and

sedimentary rocks, which inherently contribute to higher radionuclide concentrations [22]. These formations act as natural sources, releasing radionuclides into the surrounding soil and environment. Industrial activities in Anambra state further amplify these concentrations. The state's industries, including mining, manufacturing, and construction, play a pivotal role in redistributing radionuclides through processes such as raw material extraction and processing. For instance, mining and quarrying activities disturb subsurface materials, mobilizing radionuclides such as ^{40}K, ^{238}U, and ^{232}Th. Additionally, industrial emissions, waste disposal, and the use of by-products in construction and land reclamation contribute to the elevated observed radionuclide activity levels [23].

In comparison with other studies, significantly higher ^{40}K activity levels were recorded in this study for Imo (761.29 Bq kg^{-1}) and Anambra (835.80 Bq kg^{-1}) states compared to previous studies (Table 3). This increase may be attributed to the agricultural practices of using potassium-rich fertilizers and the environmental legacy of the civil war, which could have redistributed potassium-bearing materials in these regions due to soil disturbances caused by explosives and other military activities. Interestingly, the present study recorded lower activity levels for Imo state (^{238}U: 19.19 Bq kg^{-1}, ^{232}Th: 9.30 Bq kg^{-1}), while Anambra had 21.05 Bq kg^{-1} (^{238}U) and 12.99 Bq kg^{-1} (^{232}Th). These values are lower than those reported in other southern Nigerian regions affected by the civil war, such as Ebonyi (^{238}U: 88.22 Bq kg^{-1}, ^{232}Th: 80.26 Bq kg^{-1}) and Abia (^{238}U: 52.64 Bq kg^{-1}, ^{232}Th: 97.68 Bq kg^{-1}) states. These lower values could be attributed to natural geological variability, as these areas may lack uranium and thorium-rich rocks or minerals. Over time, soil erosion and leaching, exacerbated by the post-war environmental recovery, might have further reduced the concentrations of these radionuclides. Previous studies largely did not report or detect ^{137}Cs at some locations, possibly due to its low concentrations being below detection limits (BDL) or minimal historical inputs. In the present study, the detection of ^{137}Cs (5.39 Bq kg^{-1} in Imo state and 3.88 Bq kg^{-1} in Anambra state) suggests anthropogenic contributions, likely from fallout associated with explosives used during the war [13]. The civil war may also have played a role in redistributing this radionuclide, as military activities could have introduced or concentrated cesium isotopes in localized areas.

TABLE 1. Activity concentrations of radionuclides in soil samples from Anambra.

Location	^{40}K (Bqkg^{-1})	^{238}U (Bqkg^{-1})	^{232}Th (Bqkg^{-1})	^{137}Cs (Bqkg^{-1})	D (nGyh^{-1})	AEDE (mSvy^{-1})
AN1	1223.98±5.62	27.16±5.42	5.95±0.67	BDL	67.28	0.08
AN2	1256.66±8.37	29.55±3.67	5.41±0.70	BDL	69.41	0.09
AN3	1435.33±8.33	29.73±2.93	38.69±0.53	BDL	97.62	0.12
AN4	1145.86±8.63	17.85±4.57	36.66±0.88	BDL	78.80	0.10
AN5	958.7±4.85	19.35±3.58	4.78±0.92	4.15±0.13	51.89	0.06
AN6	900.00±5.34	22.00±2.72	13.00±1.12	BDL	55.77	0.07
AN7	850.00±15.65	21.00±5.69	13.00±0.78	BDL	53.22	0.07
AN8	820±11.04	20.50±3.96	12.50±0.73	BDL	51.43	0.06
AN9	870.00±10.83	21.50±2.77	13.5.00±0.44	BDL	54.60	0.07
AN10	840.00±7.83	21.00±3.56	13.00±0.69	BDL	52.80	0.07
AN11	860.00±14.49	21.50±2.08	13.50±0.76	BDL	54.18	0.07
AN12	830.00±13.78	20.50±1.86	12.50±0.93	BDL	51.85	0.06
AN13	2135.74±15.67	57.56±3.52	8.26±1.44	3.66±0.62	120.78	0.15
AN14	880.00±14.98	22.00±3.52	13.50±1.32	BDL	55.24	0.07
AN15	810.00±6.33	20.50±3.77	12.50±0.76	BDL	51.01	0.06
AN16	890.00±6.72	22.00±1.99	13.50±0.56	BDL	55.66	0.07
AN17	800.00±5.84	20.00±1.07	12.00±0.34	BDL	50.05	0.06
AN18	870.00±3.07	21.50±1.92	13.50±0.39	BDL	54.56	0.07
AN19	850.00±11.88	21.00±2.44	13.00±0.66	BDL	53.22	0.07
AN20	820.00±10.62	20.50±2.38	12.50±0.43	BDL	51.43	0.06
AS21	763.45±6.07	9.09±1.67	9.16±0.39	BDL	41.73	0.05
AS22	664.64±14.79	10.01±3.85	5.16±0.74	BDL	35.54	0.04
AS23	566.44±7.27	29.34±2.17	7.16±0.42	BDL	41.62	0.05
AS24	567.44±8.05	20.30±1.75	8.16±0.31	BDL	38.11	0.05

Location	^{40}K ($Bqkg^{-1}$)	^{238}U ($Bqkg^{-1}$)	^{232}Th ($Bqkg^{-1}$)	^{137}Cs ($Bqkg^{-1}$)	D ($nGyh^{-1}$)	AEDE ($mSvy^{-1}$)
AS25	785.26±12.02	14.68±3.36	7.41±0.73	BDL	44.13	0.05
AS26	623.66±10.62	10.95±2.44	27.93±0.74	BDL	48.41	0.06
AS27	519.11±6.07	19.95±1.37	12.17±0.88	BDL	38.42	0.05
AS28	691.10±14.79	11.89±3.52	6.97±0.92	BDL	38.64	0.05
AS29	820.00±7.27	20.50±3.77	12.50±1.12	BDL	51.42	0.06
AS30	2084.04±8.05	28.05±1.99	14.45±1.32	BDL	108.84	0.13
AS31	860.00±4.85	21.50±1.85	13.50±0.43	BDL	54.18	0.07
AS32	2275.54±5.34	17.77±3.85	17.23±0.39	3.68±0.10	113.80	0.14
AS33	561.35±15.65	20.50±2.17	12.50±0.69	BDL	40.64	0.05
AS34	251.04±13.78	22.00±1.99	13.50±0.76	3.76±0.11	29.02	0.04
AS35	252.58±15.67	20.50±1.07	12.50±0.93	4.12±0.11	27.77	0.03
AS36	310.36±14.98	22.00±1.92	13.50±0.88	BDL	31.49	0.04
AS37	225.85±6.33	22.00±2.44	12.00±0.92	BDL	27.04	0.03
AS38	270.91±5.62	21.50±2.38	13.50±1.12	3.66±4.16	29.61	0.04
AS39	250.41±8.37	13.63±1.85	14.43±0.56	4.16±0.20	25.70	0.03
AS40	42.44±6.72	9.09±1.99	4.78±0.34	BDL	8.94	0.01
Mean	835.80±7.40	21.05±3.65	12.99±0.85	3.88±0.10	52.65	0.06

TABLE 2. Activity concentrations of radionuclides in soil samples from Imo.

Location	^{40}K ($Bqkg^{-1}$)	^{238}U ($Bqkg^{-1}$)	^{232}Th ($Bqkg^{-1}$)	^{137}Cs ($Bqkg^{-1}$)	D ($nGyh^{-1}$)	AEDE ($mSvy^{-1}$)
IN1	1435.32±6.72	27.16±5.42	8.69±0.48	BDL	77.80	0.10
IN2	1413.75±18.37	34.44±3.67	14.25±1.14	BDL	83.71	0.10
IN3	1289.09±3.07	13.63±2.93	13.2±0.84	BDL	68.25	0.08
IN4	1191.44±5.84	16.18±4.57	4.98±0.88	BDL	60.25	0.07
IN5	1145.86±10.62	14.68±3.58	6.66±0.82	BDL	58.70	0.07
IN6	1092.72±3.33	11.38±2.72	9.25±0.54	BDL	56.57	0.07
IN7	940.99±11.88	29.34±5.69	7.44±0.77	BDL	57.42	0.07
IN8	716.22±10.02	15.75±3.96	4.96±0.34	BDL	40.22	0.05
IN9	638.54±2.33	13.53±2.77	6.33±3.35	BDL	36.81	0.05
IN10	562.44±6.33	28.08±3.56	7.16±0.72	4.48±0.23	40.87	0.05
IN11	540.61±7.22	22.27±2.08	9.52±0.8	BDL	38.74	0.05
IN12	516.11±1.76	19.91±1.86	8.25±0.71	6.57±0.31	35.84	0.04
IN13	458.76±2.92	20.7±1.37	5.72±0.61	BDL	32.25	0.04
IN14	439.88±7.22	10.95±3.52	9.17±0.42	BDL	29.10	0.04
IN15	394.02±3.81	19.31±3.77	14.87±0.13	6.18±0.25	34.59	0.04
IN16	338.92±5.97	27.73±1.99	10.25±0.43	BDL	33.31	0.04
IN17	301.26±4.69	20.3±1.07	6.07±0.89	BDL	25.71	0.03
IN18	299.88±10.97	18.39±1.92	15.43±1.05	BDL	30.58	0.04
IN19	277.56±2.92	12.6±2.44	6.45±1.29	BDL	21.40	0.03
IN20	274.45±14.98	22.53±2.38	15.38±2.84	BDL	31.40	0.04
IS21	2135.74±18.37	34.44±1.85	15.43±3.73	BDL	114.56	0.14
IS22	243.96±2.17	11.86±3.85	14.43±4.72	4.97±0.29	24.61	0.03
IS23	106.01±11.02	28.05±2.17	6.63±3.03	BDL	21.50	0.03
IS24	106.01±2.97	10.01±1.92	4.96±4.03	BDL	12.13	0.02
IS25	623.66±3.77	10.01±3.36	7.93±3.54	3.89±0.11	35.56	0.04
IS26	2135.74±2.33	19.09±2.93	8.22±1.05	BDL	102.99	0.13
IS27	1614.74±6.33	11.88±4.57	11.25±1.29	BDL	79.81	0.10
IS28	277.56±3.07	12.6±3.58	6.45±2.84	BDL	21.40	0.03
IS29	716.22±5.84	15.75±2.72	4.96±1.29	BDL	40.22	0.05
IS30	439.88±10.62	10.95±5.69	9.17±2.84	BDL	29.10	0.04
IS31	550.61±10.87	22.27±3.96	9.52±0.34	7.12±0.42	39.16	0.05
IS32	516.11±10.02	22.36±1.85	8.25±3.35	3.76±0.11	36.98	0.05
IS33	1092.72±2.33	11.38±3.85	9.25±0.72	BDL	56.57	0.07
IS34	338.92±6.33	27.73±2.17	8.39±0.8	BDL	32.15	0.04
IS35	1614.74±2.33	11.88±1.99	11.25±0.71	BDL	79.81	0.10
IS36	1289.09±6.33	13.63±1.07	9.10±0.61	BDL	65.71	0.08
IS37	274.45±7.22	22.53±2.38	9.29±0.42	BDL	27.62	0.03

Location	^{40}K (Bqkg^{-1})	^{238}U (Bqkg^{-1})	^{232}Th (Bqkg^{-1})	^{137}Cs (Bqkg^{-1})	D (nGyh^{-1})	AEDE (mSvy^{-1})
IS38	1413.75±1.76	34.44±1.85	8.71±0.13	BDL	80.27	0.10
IS39	299.88±2.92	18.39±3.85	9.87±0.43	BDL	27.13	0.03
IS40	394.02±7.22	19.31±2.17	14.87±3.03	6.15±0.27	34.59	0.04
Mean	761.29±6.63	19.19±2.97	9.30±1.52	5.39±0.25	46.38	0.06

TABLE 3. Comparison of mean radioactivity levels and radiological parameters with previous studies.

Location	^{40}K (Bqkg^{-1})	^{238}U (Bqkg^{-1})	^{232}Th (Bqkg^{-1})	^{137}Cs (Bqkg^{-1})	D (nGyh^{-1})	AEDE (mSvy^{-1})	Reference
IMSU, Imo State	91.63	20.32	22.55	-	26.86	33.1	Eke *et al.* [24]
Ebonyi State	202.18	88.22	80.26	BDL	97.67	0.24	Ubgede *et al.* [25]
Abia State	179.15	52.64	97.68	-	92.45	0.11	Agbalagba *et al.* [26]
Imo State	761.29	19.19	9.30	5.39	46.38	0.06	Present Study
Anambra State	835.80	21.05	12.99	3.88	52.65	0.06	Present Study
World Average	400	35	30	59	55	1.00	UNSCEAR

Spatial distribution of radionuclide concentration within the study area, illustrated in Figs. 2(a)-2(d), revealed distinct patterns influenced by both natural and anthropogenic factors. ^{40}K concentrations ranged from 486.49 to 1205.51 Bq kg^{-1}, with the highest values observed in southern parts of Anambra and Imo states, as seen in Fig 2(a). This likely reflects the use of potassium-based fertilizers and naturally potassium-rich soils. Figure 2(b) shows that ^{238}U exhibited a narrower range (15.26–26.20 Bq kg^{-1}) and a more uniform distribution, suggesting minimal geological variability in uranium-rich materials. ^{232}Th concentrations, depicted in Fig. 2(c) varied from 8.79 to 27.97 Bq kg^{-1}, with higher levels concentrated in specific northern and central regions, likely due to thorium-rich mineral deposits. In contrast, ^{137}Cs [Fig. 2(d)] showed lower activity concentrations (0.19–6.90 Bq kg^{-1}) but notable hotspots in central regions, which may be linked to anthropogenic sources, including fallout from explosive weapons and redistribution during the civil war.

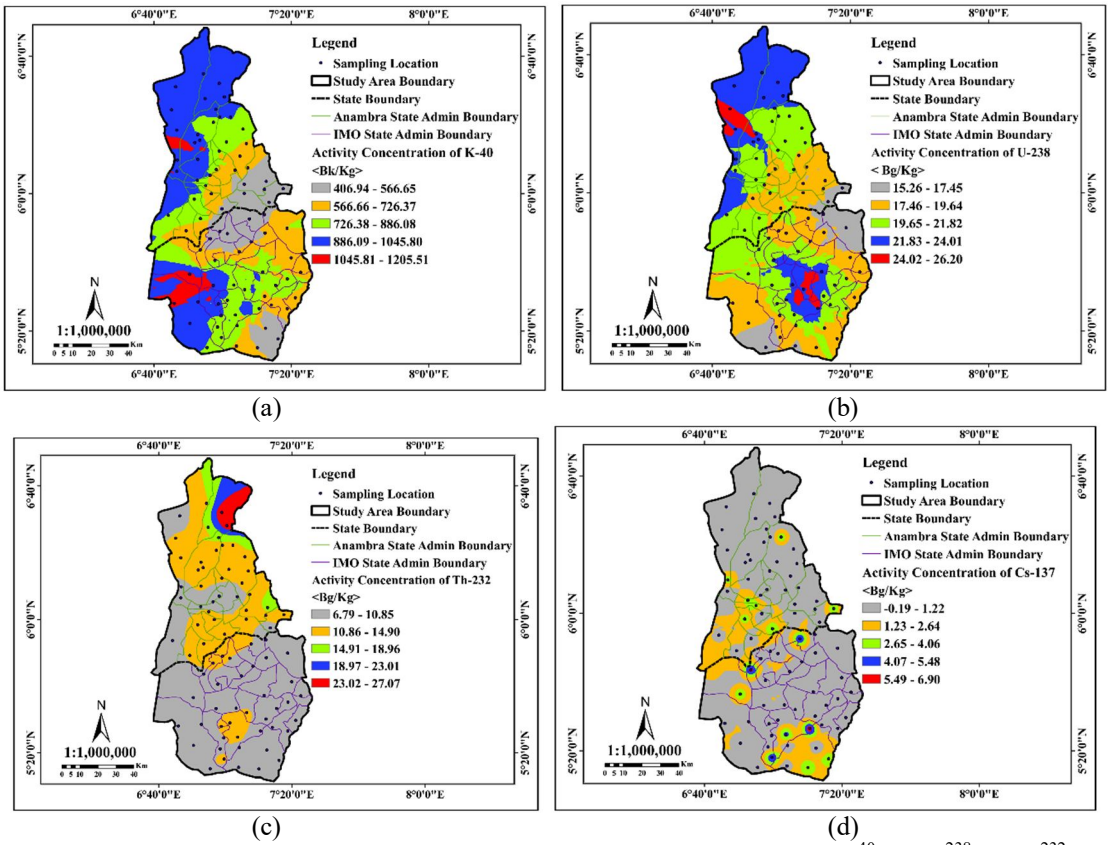

FIG. 2. Spatial distribution of radionuclide concentration within the study area: (a) ^{40}K, (b) ^{238}U, (c) ^{232}Th, (d) ^{137}Cs.

This highlights the distinct influence of human activities on cesium distribution compared with naturally occurring radionuclides. Among the radionuclides, ^{40}K showed the widest range and highest concentrations, reflecting significant variability, while ^{238}U exhibited the least spatial variability. The observed concentrations of ^{137}Cs emphasize the lingering impacts of historical events, contrasting with the geological control seen in ^{232}Th. These patterns not only highlight the environmental heterogeneity of the study area but also underscore the importance of monitoring radionuclides with both natural and anthropogenic origins for radiological safety. While the activity concentrations remain within global safety limits, elevated levels of ^{137}Cs in hotspots may require further investigation to assess localized risks.

In addition, as presented in Tables 1 and 2, the estimated average dose rate (D) values ranged from 25.431 to 120.78 nGyh^{-1} for Anambra and from 21.40 to 102.99 nGyh^{-1} for Imo, with an average of 52.65 and 46.38 nGyh^{-1}, respectively. Both mean values are below the global average of 55 nGyh^{-1} recommended by [1]. Similarly, the annual effective dose equivalent (AEDE) ranged from 0.03 to 0.15 mSvy^{-1} in Anambra and from 0.03 to 0.13 mSvy^{-1} in Imo, with mean values of 0.06 and 0.06 mSvy^{-1}, respectively. The mean values are significantly lower than the recommended 1.00 mSvy^{-1} [1]. These values indicate no significant health risks. When compared with previous studies (Table 3), the present study recorded lower absorbed dose rates, D, with corresponding AEDE values, than those reported for Ebonyi state (97.67 nGyh^{-1}, 0.24 mSvy^{-1}) and Ota, Ogun state (109.8 nGyh^{-1}, 0.135 mSvy^{-1}). This is consistent with the reduced ^{238}U and ^{232}Th activity concentrations observed in the present study areas. Furthermore, the low AEDE values are well below the global safety threshold of 1 mSvy^{-1}, indicating minimal radiological risk. The present study highlights elevated ^{40}K activity linked to agricultural and war-related soil disturbances, lower ^{238}U and ^{232}Th concentrations due to geological and environmental recovery factors, and the detection of ^{137}Cs, which was not accounted for in previous studies, likely due to its anthropogenic origins and redistribution from historical events. Despite these variations, radiological risks remain minimal in the studied regions.

4. Conclusion

Using gamma-ray spectrometry with a thallium-activated sodium iodide [NaI(Tl)] detector, the study analyzed 80 random soil samples collected from various locations within the Anambra and Imo states. The radionuclides measured include ^{40}K, ^{238}U, ^{232}Th, and ^{137}Cs, providing insight into both natural and anthropogenic radiation sources. The spatial distribution map created using ArcMap version 10.8.2 visualized the variability of radionuclide activity levels within the study area. In both states, the activity levels of the identified radionuclides, with the exception of ^{40}K, were found to be lower than the global average. The spatial distribution of the radionuclides within the study area revealed distinct patterns influenced by both natural and anthropogenic factors, with ^{40}K exhibiting the highest variability, driven by agricultural activities and naturally potassium-rich soils, while ^{238}U and ^{232}Th were predominantly influenced by geological conditions. Elevated ^{137}Cs concentrations in localized hotspots highlight anthropogenic sources such as explosive fallout and redistribution used during the civil war. Furthermore, the radiological indices estimated in lieu of the activity concentrations were lower than the permissible limit of 1.00 mSvy^{-1} recommended globally, indicating the safety of using these soil samples for their intended purposes and posed no radiological health risk. Based on the findings of the study, it is hereby recommended that other environmental matrices, such as water and plants, in the studied locations be investigated to ascertain their radiological status.

References

[1] United Nations Scientific Committee on the Effects of Atomic Radiation (UNSCEAR), "Report of UNSCEAR to the general assembly", (United Nations, New York, USA, 2000).

[2] Akinloye, M.K., Isola G.A., and Ayanlola, P.S., Int. J. Sci. Res. Pub., 8 (8) (2018) 628.

[3] Isola, G.A., Oni, O.M., Akinloye, M.K., and Ayanlola P.S., Int. J. Sci. Res. Pub., 8 (8) (2018) 618.

[4] Isola, G.A., Akinloye, M.K., Amuda, D.B., Ayanlola, P.S., and Fajuyigbe A., Int. J. Sci. Res. Pub., 10 (9) (2019) 1647.

[5] United Nations Scientific Committee on the Effects of Atomic Radiation, Sources and Effects of Ionizing Radiation, "Report to the General Assembly with Scientific Annexes". (New York, NY, USA, 2008).

[6] Manigandan, P.K. and Chandar, S.B., J. Rad. Res. Appl. Sci., 7 (2014) 310.

[7] Ekong, G., Akpa, T., Umaru, I., Lumbi, W., Akpanowo, M., and Benson, N., Int. J. Environ. Monit. Anal. 7 (2) (2019) 40.

[8] Leal, A. et al., J. Environ. Radioact., 211 (2020) 106046.

[9] Sirin, M., Microchem. J., 152 (2020) 104349.

[10] Addo, M.A., Lomotey, J.S., Osei, B., and Appiah, K., Radiat. Prot. Environ., 43 (2020) 6.

[11] Nagathil, N., Vadakkemattathil, V., Parambil, S.K., and Vamanan, P., Radiat. Prot. Dosimetry, 199 (20) (2023) 2554.

[12] Abu-Kharma, M., Rawashdeh, S., and El-Hasan, T., Int. J. Plant Anim. Environ. Sci., 14 (2024) 12.

[13] Akinloye, M.K., Isola, G.A., and Oladapo, O.O., Environ. Natl. Resour. Res., 2 (1) (2012) 140.

[14] Agbelusi, O.I., Ayanlola, P.S., Akinlabi, I.A., Amusat, T.A., Amuda, D.B., and Isola, G.A., Niger. J. Theor. Environ. Phys., 2 (2) (2024) 76.

[15] Xinwei, L., Lingquig, W., Xiaodan, J., and Leipengy, G.D., Chin. Rad. Prot. Dos., 118 (3) (2006) 352.

[16] Gao, J., Cao, C., Luo, Z., and Zhang, X., Indoor Built Environ., 23 (2014) 236.

[17] The 17 Goals of the United Nations Sustainable Development, https://sdgs.un.org/goals, Retrieved 3 September 2024.

[18] National Population Commission (NPC), "Nigeria Population 2022", (Demographics, Maps, Graphs), worldpopulationreview.com. Retrieved 3 September 2022.

[19] National Bureau of Statistics (NBS), (Demographic Statics Bulletin, 2020).

[20] Adeoje, E.A., Isola, G.A., Ayanlola, P.S., Lawal, M.K., Aremu, A.A., Oni, E.A., and Agbelusi, O.I., E-Proc. Int. Conf. Adv. Cem. Concr., 2023 (2023) 53.

[21] Awokoya, S.O., Ayanlola, P.S., Olatunji, A., Ojeniyi, F.A., Agbelusi, O.I., Orodiran, O.T, and Isola, G.A., Malays. J. Sci. Adv. Technol., 4 (4) (2024) 464.

[22] Ejeh, O.I., Heliyon, 7 (10) (2021) e08110.

[23] Onwuka, S.U., Duluora, J.O., and Amaechi, I.E., Albanian J. Agric. Sci., 12(2) (2013) 229.

[24] Eke, B.C., Akomolafe, I.R., Ukewuihe, U.M., and Onyenegecha, C.P., Environ. Health Inspect., 18 (2024).

[25] Ugbede, F.O., Osahon, O.D., and Akpolile, A.F., Environ. Forensics, 23 (1–2) (2021) 32.

[26] Agbalagba, E.O., Chaanda, M.S., and Egarievwe, S.U., Int. J. Env. Anal. Chem., 103 (17) (2021) 5539.